Role of Methionine 56 in the Control of the Oxidation−Reduction Potentials of the *Clostridium beijerinckii* Flavodoxin: Effects of Substitutions by Aliphatic Amino Acids and Evidence for a Role of Sulfur−Flavin Interactions[†]

Lawrence J. Druhan and Richard P. Swenson*

Department of Biochemistry, The Ohio State University, Columbus, Ohio 43210

Received April 6, 1998; Revised Manuscript Received May 13, 1998

ABSTRACT: Flavodoxins are small electron transferases that participate in low-potential electron transfer pathways. The flavodoxin protein is able to separate the two redox couples of the noncovalently bound flavin mononucleotide (FMN) cofactor through the differential thermodynamic stabilization or destabilization of each of its redox states. In the flavodoxin from *Clostridium beijerinckii*, the sulfur atom of methionine 56 is in direct contact with the *re* or inner face of the isoalloxazine ring of the FMN cofactor. In this study, evidence was sought for a possible role for sulfur−aromatic (flavin) interactions in the regulation of one-electron reduction potentials in flavoproteins. Met56 was systematically replaced with all the naturally occurring aliphatic amino acids by site-directed mutagenesis. Replacement of Met56 with alanine or glycine increased the midpoint potentials at pH 7 for the oxidized−semiquinone couple by up to 20 mV compared to that of the wild type, while replacement by the longer chain aliphatic residues decreased the midpoint potential by >30 mV. The midpoint potential for the semiquinone−hydroquinone couple was less negative than that for the wild type for all the mutants, increasing by as much as 90 mV for the M56I mutant. For the M56A mutant, the loss of ∼0.5 kcal/mol in the binding energy for oxidized FMN and an increase of 1.6 kcal/mol for the flavin hydroquinone, relative to that of the wild type, are responsible for the observed changes in the midpoint potentials. The stability of the semiquinone complex of this mutant was not affected. The one-election reduction potentials for the M56L, M56I, and M56V mutants are also influenced by the differential stabilization of the three redox states; however, the semiquinone complex was significantly less stable in these proteins. These differences are likely the consequence of the introduction of additional steric factors and an apparent structural preference for a smaller or more flexible side chain at this position in the semiquinone complex. While the other factors may contribute, it is argued that the results obtained for the entire group of mutants are consistent with the elimination of important sulfur−flavin interactions that contribute in part to the stabilization of the oxidized and destabilization of the hydroquinone states of the cofactor in this flavodoxin. The results of this study also demonstrate unequivocally the functional importance of this methionine residue and that it is unique among the aliphatic amino acids in its capacity to generate the physiologically relevant low reduction potential exhibited by the *C. beijerinckii* flavodoxin.

Flavodoxins are small (M_r < 20 kDa), low-potential electron transferases that undergo oxidation−reduction at a single, noncovalently bound flavin mononucleotide (FMN)[1] cofactor. This family of flavoproteins has been extensively investigated, and a large body of biophysical and biochemical information is available (*1*). All three oxidation states of the bound FMN—the oxidized (OX), one-electron reduced semiquinone (SQ), and two-electron reduced hydroquinone (HQ)—can be observed in these proteins. The blue neutral form of the flavin semiquinone is thermodynamically stabilized, while the anionic hydroquinone is destabilized primarily through unfavorable electrostatic interactions with the surrounding protein environment (*2*−*4*). As a consequence, both redox couples of the FMN cofactor are well separated in the flavodoxin and each couple can be studied separately.

One of the first and most thoroughly studied flavodoxins structurally is that isolated from *Clostridium beijerinckii*, for which the X-ray crystal structure has been solved in all three oxidation states at high resolution (*5*−*7*). As in all flavodoxins, two polypeptide loops provide most of the interactions with the isoalloxazine moiety of the FMN. One of these loops, comprised of residues 56−59, forms a unique turn in which the peptide bond between residues 57 and 58 adopts a mixture of both the typical *trans* and the unusual *cis* conformation in the oxidized state (*7*, *8*). Furthermore, during reduction to the semiquinone, the carbonyl group of

[†] This study was supported in part by Grant GM36490 from the National Institutes of Health.

* To whom correspondence should be addressed: Department of Biochemistry, 776 Biological Sciences Bldg., The Ohio State University, 484 W. 12th Ave., Columbus, OH 43210-1292. Telephone: (614) 292-9428. Fax: (614) 292-6773. E-mail: swenson.1@osu.edu.

[1] Abbreviations: FMN, flavin mononucleotide; FMN_{OX} and OX, oxidized state of the FMN cofactor; FMN_{SQ} and SQ, one-electron reduced semiquinone state; FMN_{HQ} and HQ, two-electron or fully reduced hydroquinone state; $E_{ox/sq}$, midpoint potential of the ox/sq couple of the FMN; $E_{sq/hq}$, midpoint potential of the sq/hq couple; SHE, standard hydrogen electrode.

S0006-2960(98)00770-3 CCC: $15.00
Published on Web 06/19/1998

Table 1: Primary Structure and Midpoint Potential[a,b] Comparisons within the Flavodoxin Family[c]

Source	Aligned 60s Loop Sequences[d]	$E_{OX/SQ}$	$E_{SQ/HQ}$
Anacystis nidulans	G C P T **W** N V G E L	-220	-440
Anabaena 7120	G C P T **W** N I G E L	-196	-425
Klebsiella pneumoniae	G T P T **L** G D G Q L	-170	-422
Azotobacter vinelandii	G T P T **L** G E G E L	-165	-458
Megasphaera elsdenii	G C P A **M** G S E E L	-115	-372
Clostridium beijerinckii	G C S A **M** G D E V L	- 92	-399
Clostridium pasteurianum[e]	G S P S **M** G S E V	-132	-419

[a] Values reported in millivolts vs the SHE. [b] $E_{ox/sq}$ values were adjusted, using 59 mV/pH unit, such that all reported values are at pH 7.0. [c] See Ludwig and Luschinsky (*9*), and references therein. [d] The residue which interacts with the *re* face of the FMN is bold. [e] The *C. pasteurianum* primary sequence is from Fox et al. (*46*).

the conserved Gly57 residue undergoes a reorientation in which the carbonyl oxygen "flips" from a position predominantly pointing away from the flavin to one in which it can form a new hydrogen bond with the N(5)H of the blue neutral semiquinone, contributing to the stabilization of this redox state (*6*, *7*, *9*). The structural properties of the residues in the second and third positions of this turn are critical in the stabilization of the semiquinone form of the flavodoxin (*7*, *10*). Related conformational changes have also been observed in other flavodoxins (*11*−*14*), and the conserved glycine has also been shown to be influential in the stabilization of the FMN semiquinone in the flavodoxin from *Desulfovibrio vulgaris* (*15*). Significant conformational changes associated with the reduction of the cofactor to the fully reduced hydroquinone are not apparent in any of the short chain flavodoxins (*9*).

The residues adjacent to either face of the flavin isoalloxazine ring are largely conserved throughout the flavodoxin family. The outer, or *si* face, of the flavin is usually flanked by a tyrosine or tryptophan residue. In the *C. beijerinckii* flavodoxin, Trp90 appears in a nonparallel orientation with respect to the flavin ring, while in the *D. vulgaris* flavodoxin, for example, Tyr98 is coplanar. Recent studies have demonstrated the critical importance of aromatic stacking interactions with the *si* face of the FMN in the modulation of the one-electron reduction potentials of the cofactor (*4*, *15*, *16*). The inner, or *re* face, of the cofactor is usually in contact with one of three residues: tryptophan, leucine, or methionine. Those flavodoxins which have a methionine at this location generally have less negative midpoint potentials for the ox/sq couple (Table 1). In the *C. beijerinckii* flavodoxin, the sulfur atom of this methionine residue (Met56) interacts directly with the flavin ring of the cofactor and is situated directly over the edge of the *o*-xylene ring (Figure 1). Met56 is also the first residue in a four-residue reverse turn that is involved in the conformational change associated with the reduction of the FMN. Additionally, there apparently is a small oxidation state-specific conformational change in the methionine side chain (*7*).

This study was designed to investigate whether specific methionine−FMN interactions affect the one-electron reduction potentials of the cofactor and to explore the contributions, if any, of the size and structure of the side chain at this particular position in the binding site. Using oligonucleotide-directed mutagenesis, Met56 was systematically substituted with all of the naturally occurring aliphatic amino acids, including leucine, isoleucine, valine, alanine, and glycine. Because the sulfur atom of Met56 makes direct contact with the isoalloxazine ring of the cofactor, evidence was sought for the role of specific sulfur−aromatic (flavin) interactions in the regulation of one-electron reduction potentials in flavoproteins. Also, because of its location in the critical reverse turn made up of residues 56−59, this residue could influence the conformational change and/or the relative energetics of the preferred protein structures associated with the oxidized or reduced states, indirectly causing a shift in the midpoint potentials.

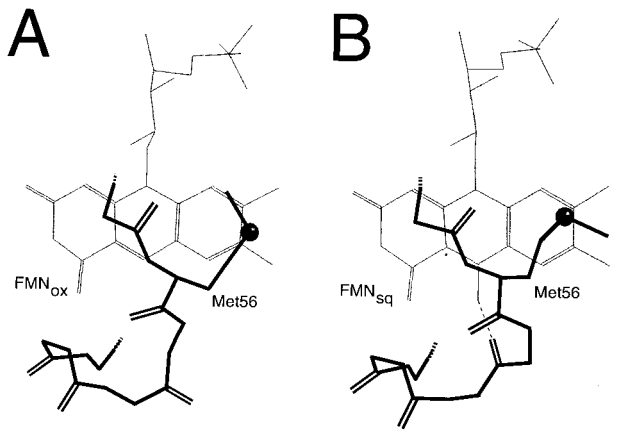

FIGURE 1: Representations of the crystal structure of the *C. beijerinckii* flavodoxin highlighting the conformations of the peptide backbone involving residues 55−60 and the side chain of Met56 in the oxidized (A) and semiquinone (B) states, viewed from the *re* face of the flavin mononucleotide cofactor. Note the change in orientation of the carbonyl of Gly57 from the O-down in the oxidized state to the O-up in the semiquinone state with the potential for the formation of a new hydrogen bond at N(5)H of the cofactor, and the slight change in the structure of the Met56 side chain. Coordinates and terminology are from Ludwig et al. (*7*).

MATERIALS AND METHODS

Materials. Indigo di- and trisulfonate were purchased from Fluka Chemicals. Benzyl viologen was obtained from Serva Chemicals. Safranine T was purchased from Fluka and recrystallized from 95% hot ethanol before being used. Flavin mononucleotide was extracted from a preparation of *C. beijerinckii* flavodoxin and purified by anion exchange chromatography. All other chemicals were of analytical reagent grade.

Bacterial Strains and Plasmids. The chemically synthesized artificial gene encoding the flavodoxin from *C. beijerinckii* (MP) was previously constructed and cloned into both the *p*KK223-3 expression vector and the phagemid *p*Bluescript (*17*). The *Escherichia coli* strains XL-1 and AG-1 were used for expression. The CJ236 strain of *E. coli* was used in the production of uracil-enriched, single-stranded DNA for mutagenesis.

Oligonucleotide-Directed Mutagenesis. The Kunkel method was used to carry out the oligonucleotide-directed mutagenesis (*18*). Single-stranded DNA was generated from the phagemid *p*BSFlasy (*p*Bluescript with the synthetic flavodoxin gene cloned into the *Eco*RI and *Hin*dIII sites) in *E. coli* strain CJ236. Two degenerate oligonucleotides were

used: 5′-ATCCTGATCCTGGGTTGCTCTGC(G)XTCG-GCGATGAAGTTC-3′ for M56L, M56I, and M56V and 5′-GGTTGCTCTGCCYZGGGCGATGAAG-3′ for M56A and M56G. The nucleotide in parentheses is a silent mutation introduced for screening purposes. The underlined nucleotides represent the mutations that introduce the desired amino acid substitutions: X indicates C, G, and A, Y indicates G and T, and Z indicates G and C. Each mutation was initially identified by restriction mapping. All of the mutants remove an *Nco*I site, M56L creates an *Hha*I site, M56I creates a *Pvu*I site, M56A creates an *Sst*II site, and M56G creates an *Nci*I site. All of the mutations were confirmed by dideoxy termination DNA sequencing using the Sequenase protocol (*19*). The second oligonucleotide also has the possibility of generating two additional mutants, M56W and M56S.

Expression and Purification of Mutant Flavodoxin Proteins. The flavodoxin structural genes for each mutant were subcloned into the *p*KK223-3 expression vector using the *Hin*dIII and *Eco*RI restriction sites and used to transform either the XL-1 Blue or AG-1 strain of *E. coli* for expression. Except for the following modification, the flavodoxin holoproteins were purified by a previously described procedure (*16*, *20*). Prior to the first anion exchange chromatographic step, nucleic acids and flavodoxin were precipitated by slowly adding a 1% (w/v) poly(ethylene imine) solution, while the mixture was being stirred on ice, to a final poly(ethylene imine) concentration of 0.15% (w/v). Flavodoxin was resolubilized from the resultant precipitate with 50 mM Tris-HCl (pH 7.0) containing 300 mM NaCl. The solubilized supernatant was diluted 3-fold with 50 mM Tris-HCl (pH 7.0) and loaded onto a DEAE anion exchange column equilibrated to pH 7.0. The flavodoxin holoprotein was eluted from the DEAE column, chromatographed on a Sephadex G-50 column, and concentrated by ultrafiltration as previously described (*3*, *20*). The Sephadex G-50 column was not used in the purification of the M56I mutant due to the tendency of the FMN to dissociate from this protein. Instead, a second anion exchange chromatography step was applied using a Bio-Rad 5 mL High Q anion exchange cartridge. The column was eluted with a 0 to 250 mM NaCl gradient at 1.5 mL/min over the course of 60 min. Fractions with an A_{272}:A_{448} ratio of $\leq$4.9 were then desalted and concentrated by ultrafiltration. All preparations were >95% pure as determined by SDS−PAGE (*21*).

UV−Visible and Fluorescence Spectroscopy. All UV−visible absorbance spectra were recorded using a Hewlett-Packard HP 8452A diode array spectrophotometer. Extinction coefficients of the fully oxidized flavodoxin holoproteins were determined using a protocol described by Mayhew and Massey with a minor modification (*22*). An extinction coefficient of 12 500 M^{-1} cm^{-1} at 445 nm was used for the determination of the FMN concentration (*23*). Fluorescence measurements were made at an excitation wavelength of 445 nm by monitoring the emission at 520 nm on a Perkin-Elmer LS50B luminescence spectrophotometer.

Determination of the One-Electron Reduction Potentials. Oxidation−reduction potentials were determined at 25 °C in 50 mM sodium phosphate (pH 7.0) as previously described (*2*). The indicator dyes (with their midpoint potentials at pH 7 and 25 °C vs the standard hydrogen electrode) used were indigo disulfonate (−116 mV), indigo trisulfonate (−75 mV), safranine T (−280 mV), and benzyl viologen (−359 mV) (*24*, *25*). The experimental error of less than ±5 mV is estimated for midpoint potential values.

Determination of the Binding Constants for FMN. The dissociation constants for the FMN_{OX} complex of the wild type and the flavodoxin mutants were determined using either ultraviolet−visible absorption spectroscopy or fluorescence spectroscopy under conditions identical to those used for the determination of the midpoint potentials. Apoflavodoxin was prepared as previously described (*3*, *26*) and titrated into a solution with a known FMN concentration until there were no further changes in the absorption spectra or fluorescence. Peak-to-valley values from ultraviolet−visible difference spectra or the fluorescence emission at 520 nm, with excitation at 445 nm, were corrected for dilution and plotted as a function of added apoflavodoxin. The dissociation constant was obtained by fitting these data to a quadratic solution of the equation describing a normal, single-site binding isotherm. The K_d values for the semiquinone and hydroquinone forms of the cofactor were determined from the linked equilibria involving the K_d for the oxidized cofactor, the determined midpoint potentials for each couple, and the published one-electron reduction potentials of Draper and Ingraham (*27*) for free FMN (*28*).

Molecular Modeling. Geometry-optimized structures for each mutant protein were generated with the following energy minimization strategy using the AMBER force field (*29*) implemented using the HyperChem modeling package (Autodesk, Inc.). In this study, the coordinates for the oxidized (3fxn) and semiquinone (4fxn) forms of the flavodoxin were used, although similar results were obtained using the coordinates reported more recently (5nll). All the residues within a 7 Å radius of the C_α of residue 56 were selected, extended to the next sp3 atom, and subjected to 100 cycles of energy minimization using the steepest descent algorithm, using a distance-dependent dielectric with a scale factor of 1, *1−4* scale factors of 0.5, and a switched cutoff with outer and inner radii of 14 and 10 Å, respectively. The minimization was completed by the application of the Polak−Ribiere conjugate gradient, using the same parameters, converging to a rms gradient end point of 0.01 kcal $Å^{-1}$ mol^{-1}. Although the FMN atoms were included in the calculation, the cofactor itself was not optimized because of the uncertainty for several parameters for the flavin molecule. Single-point energy calculations for residues of interest (extended to the next sp3 atom) were performed similarly. The solvent-exposed surface of the cofactor was determined with the Quanta software package (Molecular Simulations Inc.) using a rolling ball algorithm with a probe radius of 1.4 Å (*30*).

RESULTS

Generation, Expression, and Characterization of the Mutants. A series of five flavodoxin mutants in which Met56 was substituted with other aliphatic amino acids, including glycine, was generated by the Kunkel method of oligonucleotide-directed mutagenesis using two sets of degenerate oligonucleotide primers. The flavodoxin holoproteins were overexpressed in *E. coli* using the *p*KK223-3 expression vector and purified as the holoprotein in the fully oxidized state. A modification to our standard purification

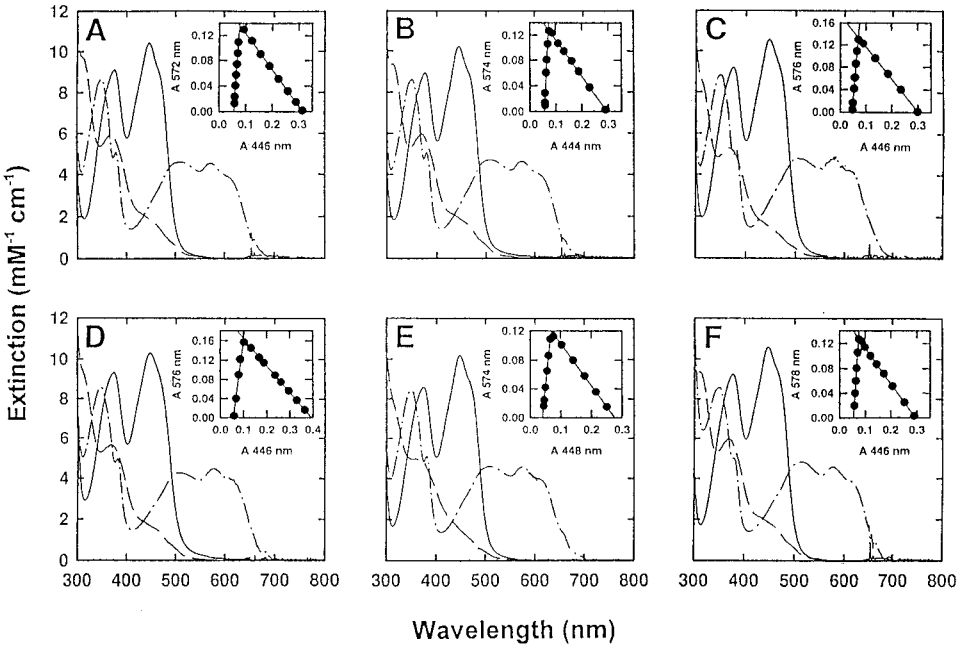

FIGURE 2: Near-ultraviolet−visible absorbance spectra of the recombinant wild-type *C. beijerinckii* flavodoxin and M56A, M56V, M56I, M56L, and M56G flavodoxin mutants (A−F, respectively) for each oxidation state as determined by anaerobic reduction with sodium dithionite. Flavodoxin in 50 mM phosphate buffer (pH 7.0) was titrated under argon in a sealed cuvette at 25 °C. In each panel, the final spectrum of the oxidized state (solid line), the blue neutral semiquinone (dot−dash line), and the fully reduced or hydroquinone (dashed line) are represented. For each mutant, the final spectrum of the semiquinone was determined by subtracting the small amount of oxidized species present near the midpoint of the titration and rescaled to 100%. Similarly, the final spectrum of the hydroquinone was determined by subtracting the spectral contributions of any semiquinone and/or excess reduced dithionite remaining at the end of the titration and rescaled. The insets are plots of the changes in absorbance in the 580 nm region (representing the λ_{max} of the semiquinone species) vs those in the 450 nm region (largely representing the oxidized species) during the course of the titration.

procedure was necessary, however, to purify the M56I mutant as the holoprotein, due to the relatively low FMN binding affinity. The A_{274}:A_{446} ratio of the final preparation of each mutant flavodoxins was 4.5 ± 0.2, similar to that of the wild type and indicative of the stoichiometric binding of the FMN cofactor.

The visible absorbance spectra of each mutant were determined in all three redox states during reductive titrations with sodium dithionite under anaerobic conditions (Figure 2). The overall spectral characteristics of each mutant remain very similar to those of the wild type in all three redox states; however, some subtle differences were noted. The λ_{max} for the oxidized flavin was shifted slightly to 448 nm in the M56L mutant, to 446 nm for M56V, M56I, and the wild type, and to 444 nm for M56A (based on the 2 nm resolution of the spectrophotometer). A shift to lower wavelengths as the size of the side chain decreases may be consistent with a slight increase in the polarity of the flavin environment. However, a concomitant shift in the λ_{max} of the second transition was not apparent, so this conclusion is somewhat tentative (*31*). The characteristics of the hydroquinone spectrum for each mutant are similar to those of the wild type. Shoulders at 450 and 310 nm and a distinct peak around 370 nm were noted. The extinction coefficient of the 370 nm peak generally decreases as the size of the side chain increases. These spectral characteristics have been interpreted as indicating a planar, anionic hydroquinone (*32*). These data are consistent with the crystal structures of other *C. beijerinckii* flavodoxin mutants, as well as that of the wild type, which indicate that the isoalloxazine ring is planar in all three oxidation states (*7*). The flavin fluorescence spectra for all the mutants were similar, with the fluorescence intensity quenched to values less than 1% of that of the free FMN as in the wild type.

Table 2: Oxidation−Reduction Midpoint Potentials[a] and FMN Dissociation Constants[b] of the Wild-Type *C. beijerinckii* and the M56X Mutant Flavodoxins

flavodoxin	K_d^{ox} (μM)	K_d^{sq} (nM)	K_d^{hq} (μM)	$E_{OX/SQ}$	$E_{SQ/HQ}$
WT	0.018 ± 0.002[c]	0.06 ± 0.01	0.42 ± 0.15	−92[e]	−399[e]
M56L	0.180 ± 0.02[d]	2.46 ± 0.8	2.10 ± 0.8	−128[f]	−345[h]
M56I	1.500 ± 0.2[d]	16.2 ± 3.5	3.30 ± 1.1	−122[f]	−308[h,i]
M56V	0.480 ± 0.02[d]	6.31 ± 1.6	2.80 ± 1.0	−127[f]	−328[h]
M56A	0.044 ± 0.008[c,d]	0.07 ± 0.03	0.03 ± 0.01	−72[f,g]	−331[h]
M56G	0.270 ± 0.03[d]	0.66 ± 0.2	0.30 ± 0.11	−84[f,g]	−326[h]

[a] Values are reported in millivolts vs the SHE at pH 7.0 and 25 °C. [b] The dissociation constants for FMN_{OX} are measured at pH 7.0 and 25 °C, and the FMN_{SQ} and FMN_{HQ} values are calculated using published FMN midpoint potential values (*27*). [c] Determined by fluorescence spectroscopy. [d] Determined by visible spectroscopy. [e] From Ludwig et al. (*7*) and this work. [f] Midpoint potentials were determined using indigo disulfonate as the redox indicator dye (*25*). [g] Midpoint potentials were determined using indigo trisulfonate as the redox indicator dye (*25*). [h] Midpoint potentials were determined using benzyl viologen as the redox indicator dye (*25*). [i] Midpoint potentials were determined using safranine T as the redox indicator dye (*25*).

Determination of the Oxidation−Reduction Potentials. The one-electron reduction potentials for both couples of the FMN cofactor for each mutant were determined at pH 7.0 and 25 °C by equilibration with redox indicator dyes with known $E_{m,7}$ values (*25*). The midpoint potentials of the ox/sq couple for M56L, M56I, and M56V were all more negative than that of the wild type, poised around −125 ± 8 mV (Table 2). The midpoint potentials for the M56A (−72 mV) and M56G (−84 mV) mutants are less negative than that of the wild type. All of these data conformed well to

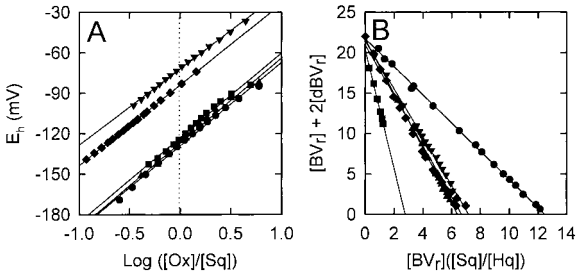

FIGURE 3: Determination of the midpoint potential for the ox/sq couple (A) and the sq/hq couple (B) for the Met56 mutants. In each case, the one-electron reduction potential was determined during anaerobic reduction with sodium dithionite by the equilibration of each flavodoxin with a redox indicator dye with a known midpoint potential in 50 mM phosphate at pH 7.0 and 25 °C. The data for the ox/sq couple are plotted according to the linear form of the Nernst equation with the system potential (E_h) determined from the distribution of the oxidized and reduced forms of the redox indicator dye. The midpoint potential for the sq/hq couple was calculated from the equilibration mixture of the flavodoxin and benzyl viologen as previously described (*2*). Symbols in each panel represent the data obtained for each flavodoxin as follows: (●) M56L, (■) M56I, (▲) M56V, (▼) M56A, and (◆) M56G.

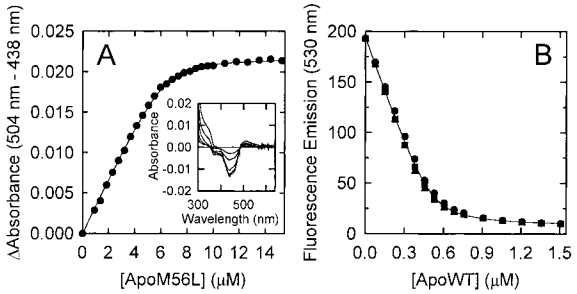

FIGURE 4: Representative determinations of the dissociation constant for the M56L mutant (A) and wild-type *C. beijerinckii* (B) flavodoxins. In each case, a solution of FMN with a known concentration was titrated with substoichiometric amounts of apoflavodoxin in 50 mM phosphate buffer at pH 7.0 and 25 °C. For the M56L flavodoxin, difference spectra were generated for each titration point (the inset shows representative difference spectra) and the peak-to-valley values were plotted as a function of the total apoprotein concentration at each point in the titration. For wild-type flavodoxin, the formation of holoprotein was monitored by the quenching of the flavin fluorescence. Each data set of spectral changes was fit to a quadratic solution to the equation describing a single binding site.

the linear form of the Nernst equation, generating slopes of 59 ± 6 mV, indicative of a one-electron equilibrium at 25 °C (Figure 3).

The midpoint potentials for the sq/hq couple of all the flavodoxin mutants, as determined by equilibration with benzyl viologen ($E_{m,7} = -359$ mV), were less negative than that of the wild type (Table 2). The M56L mutant, likely to be the most structurally conservative mutation, displayed the smallest shift from the wild-type value, increasing by 50 mV. Three mutants, M56V, M56A, and M56G, had intermediate midpoint increases of 65 ± 4 mV. Substitution with isoleucine resulted in the largest effect, increasing the midpoint by more than 90 mV to a value of −308 mV. This value, which is near the limit of the range for benzyl viologen, was confirmed using safranine T ($E_{m,7} = -280$ mV) as the redox indicator dye.

These results demonstrate that the one-electron reduction potentials of both couples are highly dependent upon the nature of the side chain at position 56. These dependencies could result from two factors, (1) the chemistry of the interaction between the side chain and each oxidation state of the cofactor and (2) the relative stability of the different protein structure found in each redox state. The contribution of each factor will be discussed in detail below. It is also important to emphasize that in no case was the midpoint potential for the sq/hq couple more negative than for the wild type.

Determination of the FMN Dissociation Constants. The dissociation constants for FMN_{OX} have been determined for each mutant by visible absorption spectroscopy or alternatively by spectrofluorimetry in the cases where values are too low to obtain reliable absorbance changes. Examples of each type of binding data are shown in Figure 4. The titration data could be fit accurately to a quadratic form of the binding isotherm as shown by the binding curves associated with each plot, generating reliable values for the dissociation constant for each mutant holoprotein. The K_d for FMN_{OX} was increased in all of the aliphatic amino acid substitutions (Table 2). The two substitutions that introduce a β-methyl group, M56I and M56V, cause the largest decrease in affinity of FMN_{OX} relative to that of the wild type, increasing the K_d to 1.5 ± 0.4 and 0.48 ± 0.02 μM, respectively, with the smaller valine side chain allowing tighter binding than the more bulky isoleucine. The M56L and M56A mutants increase the K_d to 0.18 ± 0.02 and 0.044 ± 0.008 μM, respectively, following the trend that a smaller side chain at position 56 in the *C. beijerinckii* flavodoxin favors binding of FMN_{OX}. If the side chain is completely removed, as in the M56G mutant, the binding is weakened by approximately 6-fold relative to that of the M56A mutant and 15-fold relative to that of the wild type.

Because free energy changes associated with binding are pathway-independent, a thermodynamic cycle can be employed for the calculation of the dissociation constants of both the semiquinone and hydroquinone forms of the cofactor. Such calculations require knowledge of the binding constant for the oxidized cofactor, the midpoint potentials for each redox couple for each mutant, and the established one-electron midpoint potentials for unbound FMN (*28*). The calculated values for the dissociation constants for the reduced forms of the FMN are included in Table 2. The M56A mutant binds the blue neutral FMN semiquinone very tightly, like that of the wild type, while all the rest of the mutants form significantly weaker complexes with FMN_{SQ}. In the case of M56I, the K_d for FMN_{SQ} is increased by more than 270-fold. In all cases, however, the semiquinone form of the FMN is the most tightly bound oxidation state, just as in the wild type. The FMN hydroquinone complex is typically significantly destabilized relative to the oxidized and semiquinone states in the flavodoxin, representing an important means of establishing the low reduction potentials that typify this class of flavoprotein electron transferase (*9*). This trend is generally true for this series of flavodoxin mutants. However, it is interesting to note that for the M56A and M56G mutants the hydroquinone is bound with approximately equal affinity to the oxidized state. In the case of M56A, this is accomplished by the significant improvement (by about 14-fold) in the binding of the hydroquinone relative to that of the wild type. The wild type and M56G bind FMN_{HQ} nearly equal well. The M56L, M56I, and

M56V mutants all displayed approximately 6-fold weaker binding affinities for FMN_{HQ} than the wild type (Table 2).

Molecular Modeling. Molecular modeling and molecular mechanical calculations were initiated in an attempt to gain further insight into the structural consequences of these amino acid substitutions. Given the rather conservative nature of the amino acid substitutions introduced, such calculations are likely to yield reasonably reliable indications of the highly localized structural effects. All of the mutant structures converged to similar energy values, and none of the substitutions introduced large changes in either the oxidized or the semiquinone structure. The small changes that were observed were localized within the immediate vicinity of the substitution, with no atom moving more than 1.0 Å relative to the equivalent position in the wild-type structure if applicable. These predictions are consistent with the actual three-dimensional structure data of other amino acid substitutions within this loop (*7*) and with the minor changes in the spectral properties of the bound FMN. The relative energy of each mutant in both the oxidized and semiquinone states was calculated by including only residues 55−57 in a single-point energy calculation using the AMBER force field with the same parameters used in the energy minimization calculations. The difference in conformational energies between the oxidized and semiquinone states can be used as a measure of the relative stability of the semiquinone structure for each mutant in this localized region only. Calculated differences in the single-point energies for this region between the semiquinone and the oxidized state varied from 0.2 kcal/mol for M56G to 2.2 kcal/mol for the M56L mutant, suggesting that in the absence of other nonbonding interactions a smaller side chain at position 56 favors the formation of the semiquinone structure. While one must exercise some caution in the interpretation of geometry-optimized structures, the substitutions also appear to introduce small changes in the hydrogen bond stabilizing the turn involving residues 56−59. For example, the M56A and M56G mutants seem to have slightly more favorable intraloop hydrogen bond geometry in the semiquinone state, while the M56L, M56I, and M56V mutants have slightly better hydrogen bond geometry in the oxidized state. There is also the possibility of the formation of a hydrogen bond between the carbonyl oxygen of residue 56 and the amide of residue 60. The geometry of this bond appears to remain unchanged between the oxidized and semiquinone states for M56L, M56I, and M56V. A more favorable interaction angle is apparent in the semiquinone state of the M56A and M56G mutants.

The modeled structures also suggested that changing the side chain size at position 56 could significantly affect the solvent exposure of the bound FMN cofactor. As expected, on the basis of the rolling ball algorithm (*30*), the exposed surface of the flavin systematically increased from 141 to 168 $Å^2$ (wild type vs M56G) as the size of the side chain at position 56 was decreased, with the change in exposed area being localized mainly to the *o*-xylene subnucleus of the isoalloxazine ring.

DISCUSSION

Flavodoxins serve as an exceptionally good system in which to investigate the roles of specific flavin−protein interactions in the control of the one-electron reduction potentials of the noncovalently bound FMN cofactor. The cofactor binding site provides a limited number of different types of molecular contacts with either face of the isoalloxazine ring system. The interactions are generally apolar and either aliphatic or aromatic in nature. Aromatic interactions predominate, particularly at the *si* face of the flavin, although the molecular details of these interactions are often quite different. The residue flanking the *re* face varies to a greater extent. Several flavodoxins have a methionine residue at this position, and in general, these proteins display more positive midpoint potentials, particularly for the ox/sq couple (Table 1). The structural similarities between methionine and the leucine residue found in other flavodoxins, such as that from *Azotobacter vinlandii*, raises the question of whether the unique properties of the methionine, such as the presence of the sulfur atom, play a significant role in establishing these midpoint potential differences.

The sulfur atom of Met56 in the flavodoxin from *C. beijerinckii* makes direct contact with the *o*-xylene ring of the FMN cofactor (Figure 1). Because sulfur−aromatic interactions have been identified in proteins, the strength of which varies with the properties of the aromatic ring system and geometry (*33, 34*), it is plausible that a similar interaction with the FMN cofactor could differentially stabilize or destabilize each oxidation state of the cofactor, thereby influencing the oxidation−reduction potentials in this flavodoxin. In the investigation of a role for sulfur−flavin interactions, one would ideally like to eliminate only the sulfur atom from the methionine residue without changing the rest of the structure. Limited to the naturally occurring amino acids, the methionine to leucine substitution would seem to be the most conservative, yet not perfect, replacement. In an effort to investigate this issue more precisely, we found it advantageous to replace Met56 in the *C. beijerinckii* flavodoxin not only with leucine but also with the other naturally occurring aliphatic amino acids, including glycine. Indeed, the midpoint potentials for each redox couple are seen to vary as a group by >50 mV for the ox/sq couple and by nearly 100 mV for the sq/hq couple, depending on the amino acid at this position (Table 2). These changes are particularly surprising given the rather conservative nature of these amino acid substitutions and demonstrate with certainty that Met56 plays an important role in the control of the one-electron reduction potentials in this flavodoxin. In the discussion that follows, evidence for the role of sulfur−aromatic (flavin) interactions will be presented. If the only effect of these substitutions is to eliminate a critical sulfur−flavin interaction, similar results should be obtained for each mutant. However, the differences in redox properties noted within this group suggest that, in some cases, steric or conformational effects as well as changes in the polarity and/or solvent accessibility of the cofactor binding site must also be considered in the evaluation of any putative role of the sulfur−flavin interaction. For this reason, we will initially discuss the role of sulfur−flavin interactions in the context of the methionine to alanine substitution, which is likely to introduce the fewest structural complications. The results obtained for the other aliphatic mutants allow us to exclude the effects of other types of interactions.

Scheme 1: Thermodynamic Scheme Describing the Free Energies Associated with Flavodoxin Binding of FMN in Each Oxidation State[a]

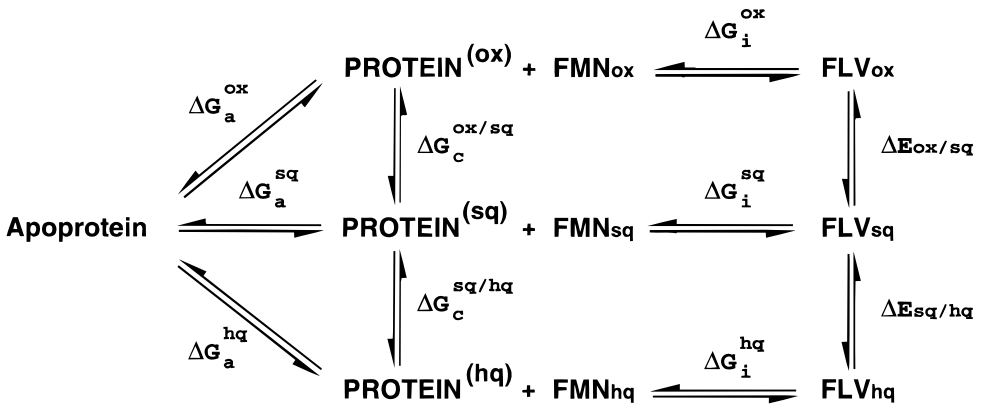

[a] See also ref *7*. Apoprotein refers to the dominant protein structure in solution lacking bound FMN. PROTEIN(ox, sq, and hq) are hypothetical or "virtual" forms of the apoflavodoxin which have the same structure as the holoflavodoxin in each oxidation state but without the bound cofactor. These forms are included to account for conformational changes associated with FMN binding (see the Discussion and also Scheme 2). FLV(ox, sq, and hq) are the final holoprotein structures in each oxidation state.

In the course of this discussion, it is necessary to separate effects that result from changes in the direct molecular interactions between the cofactor and the protein, such as the sulfur−flavin interaction, from known and probable protein conformational changes associated with cofactor binding and changes in oxidation state. We have considered a thermodynamic scheme (Scheme 1) previously formulated to assist in the interpretation of results obtained from amino acid substitutions at positions 57 and 58 in this flavodoxin (*7*). In this scheme, the term "Apoprotein" refers to the dominant apoprotein structure found in solution and the term "PROTEIN" refers to a "virtual form" of the apoprotein having the same structure as the holoprotein except lacking the bound cofactor. It is necessary to include this form to separate the effects of changes in flavin−protein interactions from those arising from protein conformational differences (see the discussion in ref *7*). From this scheme, the free energy of binding of the FMN in a given oxidation state to the apoprotein would be the sum of ΔG_i and ΔG_a, as can be seen in Scheme 2. In the simplest case where no conformational changes occur, the energy of interaction between the protein and the FMN (ΔG_i) would be directly related to the K_d for this complex in each oxidation state (i.e., $\Delta G_i = \Delta G_{K_d}$ in Scheme 2). However, protein conformational differences between the apo- and holoflavodoxin are apparent (*35*−*38*), so the second set of terms (ΔG_a^{ox}, ΔG_a^{sq}, and ΔG_a^{hq}) are required to account for any free energy differences involved for each redox state (Scheme 1). Furthermore, structural changes in this region take place during the reduction of this flavodoxin to the semiquinone state, and for this reason, free energy changes associated with this conformational change ($\Delta G_c^{ox/sq}$) must also be included (*7*). The term $\Delta G_c^{ox/sq}$ is related to ΔG_a by the difference, $\Delta G_a^{sq} - \Delta G_a^{ox}$, in this scheme (see Scheme 1). A similar term is included for the conversion of the semiquinone to the hydroquinone state, although obvious structural changes have not been observed in the wild-type flavodoxin. The midpoint potential of the bound FMN is directly proportional to the free energy difference between the two oxidation states. Any change in a midpoint potential induced by an amino acid substitution must arise from changes in the stability of either oxidation state, including changes in protein conformation

Scheme 2: Energy Diagram Illustrating the Free Energy Changes Associated with the Binding of FMN to Apoflavodoxin, Including Conformational Changes[a]

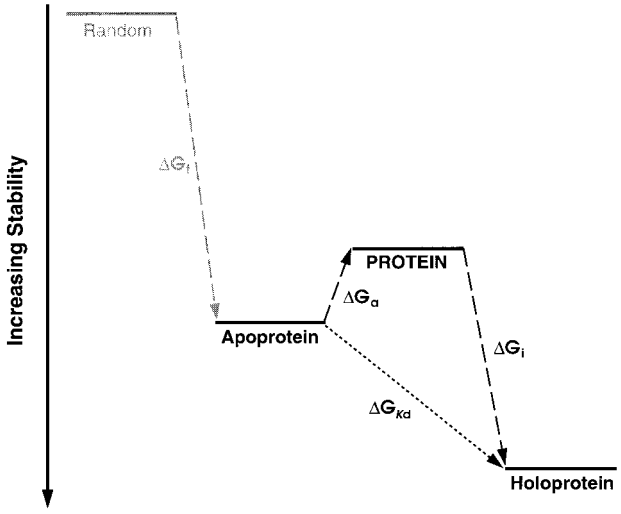

[a] Random refers to an unfolded or denatured form of the flavodoxin apoprotein. Apoprotein and PROTEIN are as described in Scheme 1, and Holoprotein represents the final holoprotein structures in each oxidation state. The free energy terms correspond to those described in Scheme 1, while the term ΔG_{K_d} is the free energy changes derived directly from the dissociation constant for FMN (i.e., $\Delta G_{K_d} = RT \ln K_d$). Note the Random to Apoprotein step is muted to emphasize its minimal effect on the binding energy due to the stability of the apoprotein structure in solution under the conditions of this study.

and in the specific FMN−protein interactions. In the case of the ox/sq couple, $\Delta E_{ox/sq}$ will be proportional to the sum $\Delta G_c^{ox/sq} + \delta\Delta G_i^{ox/sq}$, where $\delta\Delta G_i^{ox/sq} = \Delta G_i^{sq} - \Delta G_i^{ox}$. A similar relationship exists for the sq/hq couple. Of course, any structural change that affects each oxidation state equivalently, whether affecting ΔG_a and/or ΔG_i, should not alter the midpoint potentials.

The Properties of the M56A Mutant Are Consistent with a Possible Role of Sulfur−Flavin Interactions. The free energy associated with the binding of each oxidation state of the FMN cofactor was calculated from the experimentally determined dissociation constant for FMN_{OX} and the shift in midpoint potential of the flavin upon binding (Tables 2 and 3) (*28*). The overall changes in the free energy ($\Delta\Delta G$)

Table 3: Gibbs Free Energy of FMN Binding[a–c] for Wild-Type *C. beijerinckii* and the M56X Mutant Flavodoxins

flavodoxin	ΔG_{OX}	ΔG_{SQ}	ΔG_{HQ}
WT	−10.6	−13.9	−8.7
M56L	−9.2	−11.7	−7.7
M56I	−7.9	−10.6	−7.5
M56V	−8.6	−11.2	−7.6
M56A	−10.0	−13.8	−10.3
M56G	−9.0	−12.5	−8.9

[a] Values are reported in kilocalories per mole, at 25 °C. [b] The error in these values is estimated to be ±0.1−0.2 kcal/mol. [c] Values determined using $\Delta G = RT \ln K_d$.

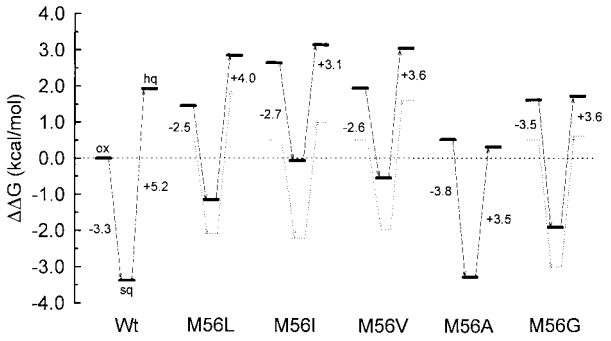

FIGURE 5: Free energy diagram comparing the relative changes in the free energy of binding for the various oxidation states of the FMN cofactor by wild-type and the Met56 mutant flavodoxins. The horizontal bars represent the differences in the free energies from that of the oxidized wild-type holoflavodoxin complex. The numbers represent the differences in the free energy of binding between the oxidized (ox) and semiquinone (sq) as well as semiquinone and hydroquinone (hq) states as indicated by the dashed lines. The free energy sets depicted by the dotted lines have been adjusted to correct for entropic (for M56G) or steric (for M56L, M56I, and M56L) factors that are expected to contribute equally to the destabilization of all three holoprotein oxidation states (see the Discussion).

associated with cofactor binding in each oxidation state versus the wild-type holoprotein in the oxidized state are depicted in the free energy diagram shown in Figure 5. Not surprisingly, significant differences are noted among these mutants. Unlike the other aliphatic mutants, $E_{ox/sq}$ for the M56A mutant is less negative than for the wild type. It is evident from the free energy diagram that this increase is primarily the result of the destabilization of the oxidized state rather than an effect on the stability of the semiquinone. The midpoint potential for the sq/hq couple for M56A is also significantly less negative than for the wild type. This increase appears to result primarily from the increased stability of the hydroquinone complex (Figure 5). What is the structural basis for these effects? The most obvious structural difference between the wild type and M56A is the removal of the dimethyl thioether moiety of the methionine side chain. The elimination of this group is expected to introduce several changes, including the elimination of any sulfur−flavin interactions, the alteration of van der Waals, hydrophobic, and steric interactions, and an increase in the solvent exposure of the flavin isoalloxazine ring, possibly increasing in the polarity of the cofactor binding site. Each will be considered in turn. However, on the basis of the collective information obtained from the analysis of all the mutants described in this study, we attribute the observed changes in the reduction potentials of the M56A at least in part to the removal of the specific sulfur−aromatic interaction between the sulfur atom of Met56 and the flavin isoalloxazine ring. This assignment will now be defended in greater depth.

Attractive electrostatic interactions between sulfur atoms and aromatic rings in proteins have been postulated (*33*, *34*). The sulfur atom apparently interacts with the quadrupole moment of the aromatic ring which is induced by the π-electron system, generating a negative electrostatic potential above and below and a positive potential along the plane of the ring (*39*, *40*). The strength of this interaction is dependent upon the degree of polarization of the aromatic ring by covalently bonded heteroatoms and the geometry of the sulfur−aromatic interaction (*34*, *40*), generating interaction energies of −0.2 to −0.75 kcal/mol in model peptides (*41*, *42*). The sulfur atom of Met56 in the *C. beijerinckii* flavodoxin (Figure 1) is adjacent to the dimethyl edge of the *o*-xylene portion of the FMN isoalloxazine ring. This location falls within the general geometric envelope for a favorable sulfur−aromatic interaction (*34*, *40*), especially when one considers the positive electrostatic surface potential of the flavin at this location as determined by ab initio calculations. This interaction should be additionally favored by the general electron deficiency of the flavin in the oxidized state (*31*). A decrease in the binding energy for the FMN_{OX} of ∼0.5 kcal/mol relative to that of the wild type is observed for the M56A mutant (Figure 5), a decrease that falls into the expected range for the elimination of a sulfur−aromatic interaction.

Furthermore, the strength of a sulfur−flavin interaction might also depend on the oxidation state of the cofactor, thereby modulating its one-electron reduction potentials. Reduction to the semiquinone increases the electron density of the FMN and is accompanied by protein conformational changes that slightly alter the sulfur−flavin interaction geometry (*7*). As the FMN becomes less electron deficient, a decrease in the attractive interactions might result, reducing the overall effect of the removal of the sulfur atom in the M56A mutant. In fact, the stability of the semiquinone complex is very similar to that of the wild-type flavodoxin (Figure 5). The addition of the second electron generates the FMN_{HQ} anion in this flavodoxin. The substantial increase in electron density along with the formation of the negative charge should further decrease any attractive sulfur−flavin interactions. Moreover, the interaction could turn repulsive, contributing to the destabilization of the hydroquinone as observed in the wild-type flavodoxin. Consistent with this premise, the FMN_{HQ} complex is, in fact, more stable in the M56A mutant than in the wild type (Figure 5). Thus, in this mutant, the increase in $E_{sq/hq}$ might result from the removal of the unfavorable sulfur−flavin interaction in this oxidation state. These arguments are, at this point, necessarily qualified by other changes associated with this substitution such as hydrophobic interactions and the solvent exposure of the FMN.

When these arguments are considered, the M56G mutant should have properties similar to those of M56A. The midpoint potentials of these mutants are very comparable (Table 2); however, somewhat surprisingly, each oxidation state in this mutant is somewhat less stable than that for M56A (Figure 5). However, if approximately 1 kcal/mol is uniformly subtracted from the free energy levels of all three oxidation states of the M56G mutant, a free energy profile very similar to that for the M56A mutant is generated (as

depicted by the profile in dotted lines for M56G in Figure 5). We attribute this nearly uniform upward shift for the M56G mutant to an effect common to all three oxidation states. Given the fact that the near absence of any side chain interactions with the FMN in both mutants is expected to affect ΔG_i equivalently in each case, a common conformational effect is implicated. While it is impossible to identify its cause with certainty, a logical explanation could be a greater conformational flexibility of the polypeptide around the glycine residue in the M56G mutant. Entropic factors would likely influence the Apoprotein structure (Scheme 1), thereby affecting each oxidation state equally by altering ΔG_a. Such changes should not alter the midpoint potentials. It is noted at this point that this similarity in the free energy profiles of the M56A and M56G mutants will be used to justify a similar adjustment in the longer chain aliphatic mutants to correct for steric factors that affect all oxidation states as will now be discussed.

The ox/sq Couple of the Longer Chain Aliphatic Amino Acid Mutants May Also Be Affected by Steric Factors. Unlike the M56A and M56G mutations, the amino acid substitutions in the M56I, M56L, and M56V mutants all result in similar substantial decreases in the midpoint potential of the ox/sq couple (Table 2). It is evident in the free energy diagram (Figure 5) that, unlike the M56A mutant, both the oxidized and semiquinone complexes are significantly less stable for these mutant proteins than for the wild type. However, the semiquinone form is stabilized (relative to the oxidized state) to a significantly lesser extent in these mutants (by ~0.7 kcal/mol) than in the wild type (−2.5 to −2.7 vs −3.3 kcal/mol, respectively), leading to the observed decreases in $E_{ox/sq}$. Also, the oxidized complex is substantially less stable than that of the M56A mutant, the free energy increasing, relative to that of the wild type, by 1.5−2.5 versus 0.5 kcal/mol. These results seem to exclude a loss of hydrophobic interactions and/or an increase in solvent exposure of the cofactor as causes of the increase observed for the M56A mutant (more on this later), strengthening the conclusion that at least part of the destabilization of the oxidized complex in all these mutants can be attributed to a loss of the favorable sulfur−aromatic interaction.

The differing structural properties of the side chains in the M56I, M56L, and M56V mutants could also introduce the destabilizing effects of steric hindrance that may contribute to the larger increases in the free energy associated with these mutants. The methionine side chain is relatively flexible and is seen to pack against the isoalloxazine ring with minimal apparent steric interference (*6*, *7*). Branched side chains should significantly reduce side chain flexibility, a β-methyl branch more so than a γ-methyl, and the extra bulk could sterically interfere with FMN binding. The introduction of a γ-methyl branched side chain (M56L) significantly reduces the stability of the holoprotein complex in the oxidized state, by 1.4 kcal/mol compared to that of the wild type (Figure 5). Comparison of the binding energies of M56L and M56I indicates that moving the methyl group to the β-position increases the destabilization of the holoprotein by an additional 1.3 kcal/mol, consistent with the introduction of greater steric hindrance by this substitution. If this is the case, the removal of side chain mass should produce tighter binding. Comparisons of the energy of binding of M56L to M56A or of M56I to M56V (both β-branched) demonstrate that a smaller side chain produces greater stability in the holoprotein complex. Thus, these data imply that steric interference is at least partially responsible for the decrease in the FMN binding affinity in the M56L, M56I, and M56V mutants. If these steric effects contribute equivalently to the destabilization of all three oxidation states of these mutants, as one might expect, they should not contribute significantly to the observed changes in midpoint potentials, however.

The application of a uniform correction to the M56L, M56I, and M56V mutants, as was done for M56G, again, by adjusting the free energy levels of the oxidized complex to be equivalent to that of M56A to accommodate a loss in any sulfur−flavin interaction, generates free energy profiles that are not entirely comparable to that of the M56A mutant (depicted by the dotted profiles for each protein). It is quite apparent that, relative to the wild-type flavodoxin, the semiquinone complex is substantially less stable in these proteins (Figure 5). Why is this? Met56 is part of the four-residue turn involved in the important conformational change associated with the thermodynamic stabilization of the semiquinone through hydrogen bonding at N(5)H of the FMN (*6*, *7*) (Figure 1). Previous studies have shown that $E_{ox/sq}$ is very sensitive to amino acid substitutions in this region. Even the rather conservative substitution of alanine for Gly57 substantially decreases $E_{ox/sq}$ without introducing significant structural changes as determined by X-ray crystallography (*7*, *8*). Such substitutions are thought to affect the energetics of this conformational change (i.e., ΔG_c) and/or influence the strength of this hydrogen bonding interaction (ΔG_i), thereby differentially altering the stability of the semiquinone state and shifting the midpoint potentials. Similar effects may also be manifested within this group of mutants. As for the Gly57 mutants, the geometry-optimized structures of the Met56 mutants in both the oxidized and semiquinone states suggest that the structural changes caused by amino acid substitutions in this region of the protein should also be rather small. The associated single-point energy calculations using these structures did suggest possible structural energy differences between the oxidized and semiquinone complexes that are dependent upon the size of the side chain at position 56 (smaller size and/or perhaps greater flexibility, favoring the semiquinone state), possibly specifying a change in $\Delta G_c^{ox/sq}$. However, our understanding of the functional consequences of the special structural characteristics of this region in this flavodoxin, including the unusual *cis* configuration of the central peptide bond, is still rather limited and requires further study (*7*).

The sq/hq Couple of the Larger Aliphatic Amino Acid Mutants. The midpoint potentials for the sq/hq couple for the M56I, M56L, and M56V mutants, like M56A and M56G, are also less negative than that of the wild type, increasing by about 90 mV for the M56I mutant. The midpoint potential for this couple is determined by the relative free energy difference between the semiquinone and hydroquinone states. This difference is similar among this group of mutants, averaging 3.6 ± 0.4 kcal/mol, a value comparable to those for M56A and M56G. All are substantially less than the 5.2 kcal/mol for the wild type (Figure 5). Is it only coincidental that this value is so similar for all these mutant, despite the substantial differences in the stability of the semiquinone complex? We think not and suggest a common

cause in all cases for the following reasons. Significant conformational differences between the semiquinone and hydroquinone states are not apparent in the wild-type protein (*6*, *7*) (i.e., $\Delta G_c^{sq/hq} = 0$ in Scheme 1); therefore, in this case, any change in ΔG_a^{sq} will likely be accompanied by an equal change in ΔG_a^{hq}. Also, any disruption of an interaction common to both the semiquinone and hydroquinone complex in these mutants, such as hydrogen bonding at N(5)H, should destabilize each to a similar extent (i.e., equivalently affecting ΔG_i^{sq} and ΔG_i^{hq}). All else being equal, it is reasonable to expect that the hydroquinone should be destabilized relative to the semiquinone by about 5.2 kcal/mol in the mutants as well, unless a common feature affects the interaction energy (ΔG_i) for either FMN_{SQ} or FMN_{HQ} by about 1.6 kcal/mol in all these mutants. While this conclusion is necessarily qualified by the differing structural properties of the amino acids involved, the data are at least consistent with the removal of the destabilizing effect of the sulfur atom adjacent to the FMN_{HQ} in these mutants just as is suggested for the M56A mutant, with the additional variability within this group possibly related to steric factors. Although more difficult to rationalize, the data do not completely exclude the effects of the alteration of some other type of interaction unique to one or both of these oxidation states, however.

Are Changes in Hydrophobic Interactions or Binding Site Polarity Affecting the Midpoint Potentials? The possibility that reduced hydrophobicity, greater solvent exposure, and/or an increase in the polarity of the FMN binding are responsible for the altered reduction potentials of the M56A and M56G mutants was raised earlier. The longer chain aliphatic mutants provide further insights on this issue. The solvent accessible surface area of the cofactor in the geometry-optimized structures, as determined by the application of a rolling ball algorithm, increases as the size of the side chain at position 56 decreases. If the hydrophobic effect is a major factor influencing FMN binding, as proposed by Janin and Chothia (*43*), M56L and M56I should bind FMN_{OX} more tightly than M56A and M56V, respectively. This is not the case (Tables 2 and 3 and Figure 5). Our results are consistent with the calorimetric work done on the *A. vinlandii* flavodoxin which indicates that hydrophobic interactions are not the thermodynamic driving force in cofactor binding (*44*) and, therefore, may not be responsible for the weaker binding of the oxidized cofactor in these mutants. Although the influence of steric factors cannot be entirely excluded, these observations provide further support for the role of sulfur−flavin interactions in this flavodoxin.

Changes in the solvent exposure of the FMN and the polarity of the binding site should exert the largest effect on the stability of the hydroquinone anion. The process of moving an ion from a polar environment to an apolar environment is endothermic (*45*); therefore, as the polarity of the binding site increases, the solvation free energy, or self-energy of the FMN_{HQ} anion, should decrease, and the hydroquinone anion−apoflavodoxin complex should become more stable. On the basis of the pattern of the FMN solvent exposure and changes in hydrophobicity introduced by each substitution, the stability of the anionic hydroquinone complex should follow the trend WT < M56L < M56I < M56V < M56A < M56G. Overall, the data do not fit very well with this trend. The largest increase in solvent exposure is expected for the M56A and M56G mutants for which the stability of the hydroquinone complex relative to the oxidized state is improved. However, because the negative charge develops during the reduction of the semiquinone to the hydroquinone anion, one expects a larger solvation effect between these two forms, but as discussed above, the free energy differences between the semiquinone and hydroquinone complexes in these mutants are not that different from those of the longer chain series. Thus, this analysis also tends to support the role of the specific sulfur−aromatic interaction rather than solvent exclusion in the destabilization of the FMN_{HQ} in this flavodoxin. These results conform to previous studies on the flavodoxin from *D. vulgaris* which also suggest that changes in solvent exposure may play a small role in affecting the reduction potential in flavodoxins; however, the destabilization of the hydroquinone anion in the flavodoxins has been attributed primarily to long-range electrostatic and aromatic stacking interactions (*2*−*4*).

Why Has "Nature" Chosen Methionine for Position 56? The evidence, taken collectively, appears to be consistent with an important role for sulfur−flavin interactions in the modulation of the one-electron reduction potentials in this flavodoxin. This conclusion is necessarily somewhat qualified because each substitution could have more than one structural consequence. However, the differing properties of each group of mutants do seem to largely exclude the effects of steric hindrance and changes in hydrophobicity and in solvent exposure and/or polarity of the cofactor binding site. Despite these qualifications, the unique functional role of Met56 in this flavodoxin is unequivocal. Flavodoxins function as low-potential electron transfer proteins, using the sq/hq couple of the FMN cofactor in vivo. Therefore, one of the primary functions of these proteins is to thermodynamically separate these two oxidation states, through either the stabilization of the FMN_{SQ}, destabilization of FMN_{HQ}, or both, generating the low one-electron reduction potential. Figure 5 graphically demonstrates that, while some mutants destabilize the FMN_{HQ} complex better than methionine (i.e., M56L, M56I, and M56V), these mutants less readily stabilize the FMN_{SQ} complex, and thus, they produce a midpoint potential that is not as negative as that of the wild type. Conversely, the semiquinone complex of M56A is just as stable as the wild type, but this mutant does not destabilize the FMN_{HQ} relative to the oxidized state. So, it is quite intriguing that methionine is the only residue of all the naturally occurring apolar aliphatic amino acids that was able to maximally stabilize the semiquinone while at the same time significantly destabilize the hydroquinone, an optimal situation for the generation of low reduction potentials for the sq/hq couple, the couple thought to be physiologically relevant in this flavodoxin. Additionally, a methionine at the *re* face of the cofactor produces a more stable holoprotein complex, ensuring saturation of the flavodoxin apoprotein at a low intracellular FMN concentration. It is not surprising, then, that a methionine residue has been retained at this position of the *C. beijerinckii* flavodoxin and perhaps the others, as it produces the lowest $E_{sq/hq}$ while maintaining reasonable cofactor binding levels. Whether these properties can be attributed primarily to a unique role of the sulfur−aromatic interaction in this flavodoxin as suggested by the data in this study and/or are the consequence of other structural or conformational aspects remains to be determined by further structural studies. It is also of interest to note

that a leucine residue adjacent to the *re* face of the FMN cofactor, as in the M56L mutant, generated a more negative $E_{ox/sq}$ value, consistent with the trend observed in the comparison of the primary sequences of the flavodoxin family (Table 1). However, the more negative midpoint potentials for the sq/hq couple observed in the other flavodoxins lacking this methionine residue must originate from other structural differences.

ACKNOWLEDGMENT

We thank Prof. Martha L. Ludwig of the University of Michigan for her insightful comments during the preparation of the manuscript.

REFERENCES

1. Mayhew, S. G., and Tollin, G. (1992) in *Chemistry and Biochemistry of Flavoenzymes III* (Müller, F., Ed.) pp 389−426, CRC Press, Boca Raton, FL.
2. Zhou, Z., and Swenson, R. P. (1995) *Biochemistry 34*, 3183−3192.
3. Zhou, Z., and Swenson, R. P. (1996) *Biochemistry 35*, 12443−12454.
4. Zhou, Z., and Swenson, R. P. (1996) *Biochemistry 35*, 15980−15988.
5. Burnett, R. M., Darling, G. D., Kendall, D. S., LeQuesne, M. F., Mayhew, S. G., Smith, W. W., and Ludwig, M. L. (1974) *J. Biol. Chem. 249*, 4383−4392.
6. Smith, W. W., Burnett, R. M., Darling, G. D., and Ludwig, M. L. (1977) *J. Mol. Biol. 117*, 195−225.
7. Ludwig, M. L., Pattridge, K. A., Metzger, A. L., Dixon, M. M., Eren, M., Feng, Y., and Swenson, R. P. (1997) *Biochemistry 36*, 1259−1280.
8. Ludwig, M. L., Dixon, M. M., Pattridge, K. A., and Swenson, R. P. (1994) in *Flavins and Flavoproteins 1993* (Yagi, K., Ed.) pp 363−366, Walter de Gruyter and Co., Berlin.
9. Ludwig, M. L., and Luschinsky, C. L. (1992) in *Chemistry and Biochemistry of Flavoenzymes III* (Müller, F., Ed.) pp 427−466, CRC Press, Boca Raton, FL.
10. Ludwig, M. L., Pattridge, K. A., Eren, M., and Swenson, R. P. (1991) in *Flavins and Flavoproteins 1990* (Curti, B., Ronchi, S., and Zanetti, G., Eds.) pp 423−428, Walter de Gruyter and Co., Berlin.
11. Watenpaugh, K. D., Sieker, L. C., and Jensen, L. H. (1976) in *Flavins and Flavoproteins 1976* (Singer, T. P., Ed.) pp 405−410, Elsevier Scientific Publishing Co., Amsterdam.
12. Laudenbach, D. E., Straus, N. A., Pattridge, K. A., and Ludwig, M. L. (1988) in *Flavins and Flavoproteins 1987* (Edmondson, D. E., and McCormick, D. B., Eds.) pp 249−260, Walter de Gruyter and Co., Berlin.
13. Luschinsky, C. L., Dunham, W. R., Osborne, C., Pattridge, K. A., and Ludwig, M. L. (1991) in *Flavins and Flavoproteins 1990* (Curti, B., Ronchi, S., and Zanetti, G., Eds.) pp 409−413, Walter de Gruyter and Co., Berlin.
14. Watt, W., Tulinsky, A., Swenson, R. P., and Watenpaugh, K. D. (1991) *J. Mol. Biol. 218*, 195−208.
15. Mayhew, S. G., O'Connell, D. P., O'Farrell, P. A., Yalloway, G. N., and Geoghegan, S. M. (1996) *Biochem. Soc. Trans. 24*, 122−127.
16. Swenson, R. P., and Krey, G. D. (1994) *Biochemistry 33*, 8505−8514.
17. Eren, M., and Swenson, R. P. (1989) *J. Biol. Chem. 264*, 14874−14879.
18. Kunkel, A. T., Roberts, J. D., and Zakour, R. A., (1987) *Methods Enzymol. 154*, 367−382.
19. Sanger, F., Nicklen, S., and Coulson, A. R. (1977) *Proc. Natl. Acad. Sci. U.S.A. 74*, 5463−5467.
20. Krey, G. D., Vanin, E. F., and Swenson, R. P. (1988) *J. Biol. Chem. 244*, 15436−15443.
21. Laemmli, U. K. (1970) *Nature 227*, 680.
22. Mayhew, S. G., and Massey, V. (1969) *J. Biol. Chem. 244*, 794−802.
23. Whitby, L. G. (1953) *Biochem. J. 54*, 437−442.
24. Michaelis, L., and Hill, E. S. (1933) *J. Gen. Physiol. 16*, 859−873.
25. Clark, W. M. (1972) *Oxidation Reduction Potentials of Organic Systems*, Robert E. Krieger Publishing Co., Huntington, NY.
26. Wassink, J. H., and Mayhew, S. G. (1975) *Anal. Biochem. 68*, 609−616.
27. Draper, R. D., and Ingraham, L. L. (1968) *Arch. Biochem. Biophys. 125*, 802−808.
28. Dubourdieu, M., LeGall, J., and Favoudon, V. (1975) *Biochim. Biophys. Acta 376*, 519−532.
29. Weiner, S. J., Kollman, P. A., Case, D. A., Singh, U. C., Ghio, C., Alagona, G., Profeta, S., Jr., and Weiner, P. (1984) *J. Am. Chem. Soc. 106*, 765−784.
30. Connolly, M. L. (1983) *Science 221*, 709−712.
31. Müller, F. (1991) in *Chemistry and Biochemistry of Flavoenzymes* (Müller, F., Ed.) Vol. I, pp 38−45, CRC Press, Boca Raton, FL.
32. Ghisla, S., Massey, V., Lhoste, J. M., and Mayhew, S. G. (1974) *Biochemistry 13*, 589−597.
33. Morgan, R. S., Tatsch, C. E., Gushard, R. H., McAdon, J. M., and Warme, P. K. (1978) *Int. J. Pept. Protein Res. 11*, 209−217.
34. Reid, K. S. C., Lindley, P. F., and Thornton, J. M. (1985) *FEBS Lett. 190*, 209−213.
35. Barman, B. G., and Tollin, G. (1972) *Biochemistry 11*, 4746−4754.
36. Dubourdieu, M., MacKnight, M. L., and Tollin, G. (1974) *Biochem. Biophys. Res. Commun. 60*, 649−655.
37. Leenders, R., van Hoek, A., van Iersel, M., Veeger, C., and Visser, A. J. W. G. (1993) *Eur. J. Biochem. 218*, 977−984.
38. Genzor, C. B., Perales-Alcon, A., Sancho, J., and Romero, A. (1996) *Nat. Struct. Biol. 3*, 329−332.
39. Hunter, C. A., and Sanders, J. K. M. (1990) *J. Am. Chem. Soc. 112*, 5525−5534.
40. Dougherty, D. A. (1996) *Science 271*, 163−168.
41. Stapley, B. J., Rohl, C. A., and Doig, A. J. (1995) *Protein Sci. 4*, 2383−2391.
42. Viguera, A. R., and Serrano, L. (1995) *Biochemistry 34*, 8771−8779.
43. Janin, J., and Chothia, C. (1978) *Biochemistry 17*, 2943−2948.
44. Carlson, R., and Langerman, N. (1984) *Arch. Biochem. Biophys. 229*, 440−447.
45. Born, M. (1920) *Z. Phys. 1*, 45−53.
46. Fox, J. L., Smith, S. S., and Brown, J. R. (1972) *Z. Naturforsch. 27B*, 1096−1100.

BI980770B